Super-resolution radial fluctuations microscopy for optimal resolution and fidelity

Contact *lin.wang@stfc.ac.uk*

Y. Li

Central Laser Facility, Research Complex at Harwell, Science and Technology Facilities Council Rutherford Appleton Laboratory, Didcot OX11 0QX, UK

L. Liu

School of Optoelectronic Engineering, Xidian University, Xi'an, Shaanxi 710071, China

S.K. Roberts

Central Laser Facility, Research Complex at Harwell, Science and Technology Facilities Council Rutherford Appleton Laboratory, Didcot OX11 0QX, UK

L. Wang

Central Laser Facility, Research Complex at Harwell, Science and Technology Facilities Council Rutherford Appleton Laboratory, Didcot OX11 0QX, UK

Introduction

Super-resolution single-molecule localization microscopy (SMLM), including stochastic optical reconstruction microscopy (STORM)[1], photoactivated localization microscopy (PALM)[2], and points accumulation for imaging in nanoscale topography (PAINT)[3], exploits the fluorescent on/off properties of suitable organic dyes and fluorescent proteins to detect single molecules at different time points. In the cases where high-density fluorescent emitters are present in SMLM, common localization algorithms may fail to precisely localize single molecules, and thereby generate significant artefacts. Alternatively, fluorescence fluctuations super-resolution microscopy (FF-SRM) is a good candidate to address this issue by exploiting the random, independent, and uncorrelated nature of fluorescence intensity fluctuations over time. FF-SRM includes, for example, super-resolution optical fluctuation imaging (SOFI), Bayesian analysis of blinking and bleaching (3B), multiple signal classification (MUSIC), and super-resolution radial fluctuations (SRRF) microscopy. Among the FF-SRM techniques, SRRF microscopy is a popular technique but is prone to artefacts, resulting in low fidelity, especially under conditions of high-density fluorophores. In this paper, we developed a novel super-resolution microscopy method, namely VeSRRF, that demonstrated superior performance in SRRF microscopy.

Method

SRRF processes raw fluorescence fluctuations images in both spatial and temporal domains. In the spatial domain, the average distance to lines of gradient around a point is measured (Fig. 1b) [4], representing the degree of convergence of the gradient. The mean convergence from the point (x_c, y_c) to the gradient line through the point (x_i', y_i') for the N ring coordinates is calculated to give the radiality of the pixel (x, y) in frame t,

$$R_t(x,y) = \frac{1}{N}\sum_{i=1}^{N} sgn(\vec{G_i}\cdot\vec{r_i})\left[1-\frac{1}{r_i}\frac{\left|(x_c-x_i')G_{yi}-(y_c-y_i')G_{xi}\right|}{\sqrt{G_{xi}^2+G_{yi}^2}}\right]^2 \quad (1)$$

where *sgn* denotes the sign function, G is the gradient, and r is the radius of the ring. Higher convergence indicates the presence of a fluorophore. In the temporal domain, the sequence of the convergence is analyzed through high-order temporal statistics, e.g., temporal radiality pairwise product mean (TRPPM), to generate a super-resolution image. TRPPM is expressed as

$$TRPPM(x,y) = \frac{2}{T(1+T)}\sum_{s=0}^{T-1}\sum_{t=s}^{T-1} R_s R_t \quad (2)$$

where T is the total number of frames, s and t enumerate the frames, and R_s and R_t are the convergences at the pixel (x, y) in frame s and t, respectively.

An enhanced version of SRRF, namely enhanced-SRRF (eSRRF), incorporates three key modifications to the original algorithm to improve image fidelity. Firstly, Fourier transform interpolation is deployed to generate subpixels, minimizing macro-pixel artefacts. Secondly, the calculation of mean convergence now employs radial gradient convergence (RGC) with a weighted factor map based on the user-defined radius R, i.e., the point spread function (PSF) size, and the intensity gradient of each pixel in the raw images. The RGC in the pixel (i_0, j_0) is

$$RGC(i_0,j_0) = \sum_{i,j}^{\Delta}\left(d\times e^{-\frac{d^2}{2\sigma^2}}\right)^4 \times \left(1-\frac{\left|G_y(i,j)\times(i-i_0)-G_x(i,j)\times(j-j_0)\right|}{d\sqrt{G_x(i,j)^2+G_y(i,j)^2}}\right) \quad (3)$$

where $\Delta = 2\sigma + 1$, σ is the standard deviation of PSF, d is the distance to the pixel of interest, and $d = \sqrt{(i-i_0)^2+(j-j_0)^2}$. Furthermore, a new parameter called sensitivity has been introduced to optimize the PSF sharpening power applied by the RGC. Lastly, the image artefact detection and quantification tool SQUIRREL is integrated to provide automated data-driven optimal parameter identification for image reconstruction, minimizing image artefacts and non-linearity.

In a different approach, the intensity and gradient variance reweighted radial fluctuations (VRRF) were independently developed to improve the imaging resolution and fidelity obtained by SRRF. As the temporal variance of intensity and gradient of a fluorophore contains its location estimation, VRRF quantitatively establishes the model of intensity and gradient fluctuations as the function of fluorophores' locations. If the image of a sample is composed of the detections of N fluorophores, the intensity distribution at the location r over time t is

$$U(r,t) = \sum_{i=1}^{N} U(r-r_i)a_i f_i(t) \quad (4)$$

where $U(r)$ is the PSF, a_i is the maximum brightness of the fluorophores, and $f_i(t)$ is the fluctuations coefficient ranging between 0 and 1. The intensity variance is expressed as

$$D[I(r)] = \sum_{i=1}^{N} U(r-r_i)^2 a_i^2 D[f_i(t)] \quad (5)$$

where $D[X]$ denotes the variance of time series X. And the gradient variance is expressed as

$$D[G(r)] = \sum_{i=1}^{N} \frac{[r-r_i]^2}{\sigma^4} U(r-r_i)^2 a_i^2 D[f_i(t)] \quad (6)$$

where σ is the standard deviation of the Gaussian function. Therefore, the intensity variance increases, but the gradient variance reduces when r approaches the center of a fluorophore (Fig. 1c). To build up the relationship between the two variances and the position of a fluorophore, the intensity weighting function is defined as

$$W(r) = \frac{D[I(r)]}{D[G(r)]} \quad (7)$$

From this equation, larger $W(r)$ values indicate a higher possibility for the centers of fluorophores. The reweighted image sequence $W(r)U(r, t)$ can then be processed using SRRF, leading

to super-resolution images with higher resolution and fewer artefacts.

In this study, we introduce the VeSRRF algorithm for FF-SRM (Fig.1). The method begins by utilizing the VRRF statistical variance analysis to perform an initial analysis on the fluorescence fluctuations image sequences. Thus, the overlapping fluorescent molecules are separated, and the artefacts caused by the high-density fluorophores can be reduced. Subsequently, the processed image sequences are further analyzed in the eSRRF algorithm. By integrating variance analysis of VRRF and eSRRF reconstruction, the VeSRRF algorithm can generate reconstructed images with optimal resolution and fidelity as the final outputs, outperforming other algorithms such as SRRF, VRRF/SRRF (referred to as VRRF for simplicity hereinafter), and eSRRF.

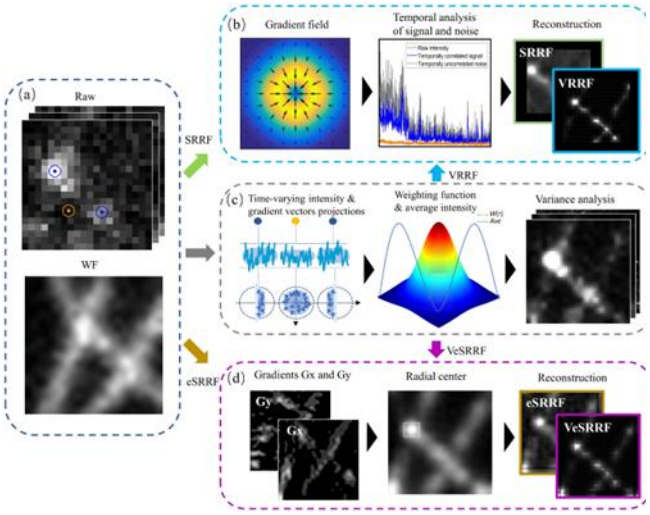

Fig. 1. Super-resolution radial fluctuations microscopy image reconstruction algorithm schematic. (a) Raw image sequence and wide-field image of microtubules. (b) SRRF reconstruction steps. (c) VRRF reconstruction steps. The reconstruction is then completed using the SRRF algorithm. (d) eSRRF reconstruction steps. The VeSRRF algorithm first processes the image sequence through VRRF, and then completes the image reconstruction using the eSRRF algorithm.

Results

Fluorescence fluctuations image series obtained under a variety of signal-to-noise ratio (SNR) conditions were also tested in SRRF, eSRRF, VRRF, and VeSRRF. As an example, dataset of Tubulin-AF488 in fixed COS7 cells was acquired using a Mercury lamp illuminator in a ZEISS microscope. In Fig. 2, from the enlarged region of interest, it was observed that the reconstructed image from VRRF showed some broken microtubule structures due to the nonlinear artefacts (Fig. 2d), which was also confirmed by the lower error mapping values from resolution scaling Pearson correlation coefficient (RSP) analysis (Fig. 2l). Next, eSRRF gave a higher RSP value but lower resolution, as depicted in Fig. 2g and 2k. In contrast, the reconstructed image from VeSRRF achieved the highest resolution and good fidelity, as shown in Fig. 2i and 2m. Finally, the quantitative QnR assessment confirmed that VeSRRF achieved optimal performance considering both resolution and fidelity, resulting in the highest QnR value. The experiment and tests showed that VeSRRF effectively super-resolved the cellular microtubule networks from fluorescence fluctuations imaging while minimizing the artefacts under conditions of high-density fluorophores.

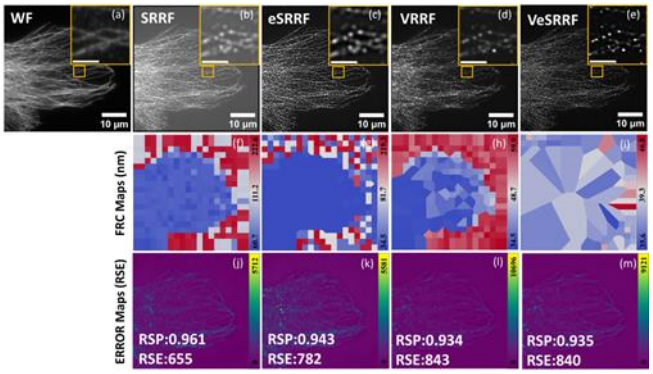

Fig. 2. Comparison of the reconstructed images of Tubulin-AF488 in fixed COS7 cells. (a) Wide-field images. (b-e) Reconstructed images from the SRRF, eSRRF, VRRF, and VeSRRF algorithms. (f-i) Corresponding FRC maps. (j-m) Corresponding error maps. Scale bar in the enlarged image of the region indicated by the yellow border box: 2 μm.

Conclusions

In this paper, we developed a novel combinatory computational super-resolution microscopy method, namely VeSRRF, that demonstrated superior performance in STORM and SRRF microscopy. We performed super-resolution image reconstructions of the simulated and experimental datasets of cellular microtubule networks under sparse and dense fluorophore conditions, and quantitatively evaluated and compared the super-resolution image quality in SRRF, eSRRF, VRRF, and VeSRRF using the FRC, RSP, and QnR metrics. Our results demonstrated that VeSRRF, the integrated VRRF and eSRRF algorithms, not only achieved the highest resolution but also produced high fidelity in the reconstructed images, outperforming other algorithms in our tests. VeSRRF conveys super-resolution, high-fidelity biological imaging using standard, inexpensive optical microscopes, common fluorophores, and simple sample preparations, making it widely applicable to any life science laboratory. VeSRRF is an exemplary method in which complementary microscopy techniques are integrated holistically, creating superior imaging performance and capabilities. We anticipate that VeSRRF will emerge as a valuable tool for many researchers to simplify their quest to solve numerous complex biological problems.

Acknowledgements

This work has been funded by the Rosetrees Trust and Stoneygate Trust grant (Seedcorn2022\100230) and by the STFC Cancer Diagnosis Network+ grant (ST/S005404/1) awarded to L.W.

References

1. Rust, Michael J., Mark Bates, and Xiaowei Zhuang. "Sub-diffraction-limit imaging by stochastic optical reconstruction microscopy (STORM)." Nature methods 3.10 (2006): 793-796.(DOI:10.1038/nmeth929)

2. Betzig, Eric, et al. "Imaging intracellular fluorescent proteins at nanometer resolution." science 313.5793 (2006): 1642-1645. (DOI: 10.1126/science.1127344)

3. Sharonov, Alexey, and Robin M. Hochstrasser. "Wide-field subdiffraction imaging by accumulated binding of diffusing probes." Proceedings of the National Academy of Sciences 103.50 (2006): 18911-18916. (DIO:10.1073/pnas.0609643104)

4. Gustafsson, Nils, et al. "Fast live-cell conventional fluorophore nanoscopy with ImageJ through super-resolution radial fluctuations." Nature communications 7.1 (2016): 12471.(DOI: 10.1038/ncomms12471)